CHEMICAL SYSTEMS LABORATORY

CONTRACTOR REPORT ARCSL-CR-83027

INFORMATION CONTENT AND SENSITIVITY OF MATRIX ELEMENTS TO STRUCTURAL CHANGES IN COMPLEX SCATTERING SYSTEM

by

William S. Bickel

A136600

20030108215

June 1983

Physics Department
University of Arizona
Tucson, Arizona 85721

DTIC
ELECTE
JAN 4 1984
B

Approved for public release; distribution unlimited.

84 01 03 001

REPORT DOCUMENTATION PAGE		READ INSTRUCTIONS BEFORE COMPLETING FORM
1. REPORT NUMBER ARCSL-CR-83027	2. GOVT ACCESSION NO.	3. RECIPIENT'S CATALOG NUMBER
4. TITLE *(and Subtitle)* Information Content and Sensitivity of Matrix Elements to Structural Changes in Complex Scattering Systems Final Report		5. TYPE OF REPORT & PERIOD COVERED Contractor Report September 1980-September 1982
		6. PERFORMING ORG. REPORT NUMBER
7. AUTHOR(s) William S. Bickel		8. CONTRACT OR GRANT NUMBER(s) DAAK 11-80-Q-0106
9. PERFORMING ORGANIZATION NAME AND ADDRESS University of Arizona Physics Department Tucson, Arizona 85721		10. PROGRAM ELEMENT, PROJECT, TASK AREA & WORK UNIT NUMBERS
11. CONTROLLING OFFICE NAME AND ADDRESS Commander Chemical Systems Laboratory Attn: DRDAR-CL'-R Aberdeen Proving Ground, Maryland 21010		12. REPORT DATE June 1983
		13. NUMBER OF PAGES 43
14. MONITORING AGENCY NAME & ADDRESS(If different from Controlling Office) Commander Chemical Systems Laboratory Attn: DRDAR-CLB-PS Aberdeen Proving Ground, Maryland 21010		15. SECURITY CLASS. (of this report) Unclassified
		15a. DECLASSIFICATION/DOWNGRADING SCHEDULE NA

16. DISTRIBUTION STATEMENT *(of this Report)*

Approved for public release; distribution unlimited.

17. DISTRIBUTION STATEMENT *(of the abstract entered in Block 20, if different from Report)*

18. SUPPLEMENTARY NOTES

Contract Project Officer: Jerold Bottiger (DRDAR-CLB-PS), (301) 671-2326

19. KEY WORDS *(Continue on reverse side if necessary and identify by block number)*

Light scattering	Polarized light scattering
Matrix elements	Optical constants
Scattering systems	Nephelometers
Light scattering curves	

20. ABSTRACT *(Continue on reverse side if necessary and identify by block number)*

Physics Department researchers at the University of Arizona investigated a number of basic problems that are central to understanding light scattered from complex systems. They started with simple geometrical systems--spherical and cylindrical geometries with known optical constants that are directly amenable to theory. Theorists can calculate exactly every scattering property (the matrix elements) of these systems and experimentalists can measure them with arbitrarily high accuracy and precision. Yet some of the most basic
(continued on reverse)

DD FORM 1473 EDITION OF 1 NOV 65 IS OBSOLETE

questions about:

    a.   the information content in the various matrix elements,

    b.   their response to large and small changes in particle property,

    c.   their specificity to a particular parameter change,

    d.   the information density per scattering angle interval,

    e.   ways to quantify changes,

still needed careful study. The research was an optical study of fundamental systems theoretically solvable and experimentally obtainable. The things learned from this study and described in this report will give insight to the matrix element data obtained from complex scattering systems.

Preface

Acknowledgements

BLANK

4

CONTENTS

BLANK

INFORMATION CONTENT AND SENSITIVITY OF MATRIX ELEMENTS TO STRUCTURAL CHANGES IN COMPLEX SCATTERING SYSTEMS

I.   STATEMENT OF THE PROBLEM AND RESEARCH ACTIVITIES

This research was carried out to investigate the basic problems that are central to understanding light scattered from complex systems. Simple systems refer to those spherical, ellip-tical and cylindrical geometries that are directly amenable to theory. Computer programs can calculate every property of these systems and can evaluate the data extracted from experimental systems. Theoretical results are known to the accuracy of the fundamental optical and electrical constants, and experimental data can be achieved to arbitrary high degree of accuracy. Laboratory devices work under ideal conditions whereas diagnostic equipment for field work is limited by (short) measurement time, angular resolution, spatial resolution, angular view (θ-scan) and time for data analysis of complex curves to get the desired information.

One problem concerns how much scattering data is needed, how good it must be and how well it describes the scatterer (or scattering system) in a practical way. Another problem concerns how much information is contained in the various light scattering matrix elements and whether changes in the signals can be related to changes in particular optical or geometrical properties. The statement of these problems and the experimental attack on them are summarized in six research objectives listed below:

A. Measure the matrix elements S_{ij} for perfect scattering systems and preparations of exactly known mixtures of perfect

7

systems. Determine which matrix elements more accurately de-
scribe the system and signify a change.

B. Procure and prepare perfect scattering systems and
exactly known mixtures of perfect systems.

C. Apply Fourier transforms, curve length, method of
moments, area ratios, inflection points, polynomial fits, etc. to
light scattering data to elucidate and quantify small changes in
the data that arise from small changes in the system.

D. Investigate the role of "average, mean or effective"
refractive index as it pertains to a complex scattering system
and determine if it is a relevant optical constant for describing
the system.

E. Investigate how much data is necessary to uniquely
determine the optical properties of a scattering system. Data
acquisition can be limited to finite angular resolution, limited
-scan, noise and imperfect optical elements. Determine what
compromises and shortcuts can be taken.

F. Prepare a tutorial report discussing the two common
systems for treating the Stoke's vector $V = (I, Q, U, V)$ and V
$= (I_e, I_r, I_q, I_v)$, the elements of the scattering matrix in each
system and the relationship between these matrices and the
experimental measurements actually made.

All research objectives have been met. Some results have
been published, some are submitted for publication and some are
in final stages of preparation (See Appendix B). The rest of this
final report will discuss some of our most important results and
show some of the data that will ultimately appear in

8

published papers.

II. THE RESULTS

We have procured and prepared perfect scattering systems and mixtures of perfect systems. These are perfect spheres (purchased from Duke Chemical Company), perfect fibers (fabricated in our laboratory), polydispersed irregular particle systems (purchased from Duke Chemical or fabricated by us), and perturbed fibers (fabricated by us). In all cases we have attempted to document the optical, electrical and geometrical properties of the particle or particle system to make the experimental data useful for theorists. This satisfies research objective B.

We have measured and calculated the matrix elements S_{ij} for perfect scattering systems and preparations of exactly known mixtures. The data were used to determine which matrix elements were needed to characterize the system and which ones were most sensitive to system changes. This satisfies research objective A. The net result is an experimental and theoretical data bank which can be manipulated and studied to examine how geometrical, optical and electrical constants contribute to the various S_{ij} light scattering curves.

The experimental and theoretical results of our studies of the above mentioned data bank and its manipulation are vast and are still being analyzed. Some results are discussed below.

A. Response of S_{ij} to Change in Particle Size.

Figures 1 through 5, which demonstrate how certain matrix elements change with particle size, is pertinent to research objective C.

9

Figure 1. The Four Non-Zero Light Scattering Matrix Elements for 0.075 Micron Spheres Showing Their Response to a One Percent Increase in Radius (Solid Line) and Their Difference $= S_{ij}^l - S_{ij}^s$ (Dotted Line) .4416λ $n_1 = 1.10$ $n_2 = 0$.

10
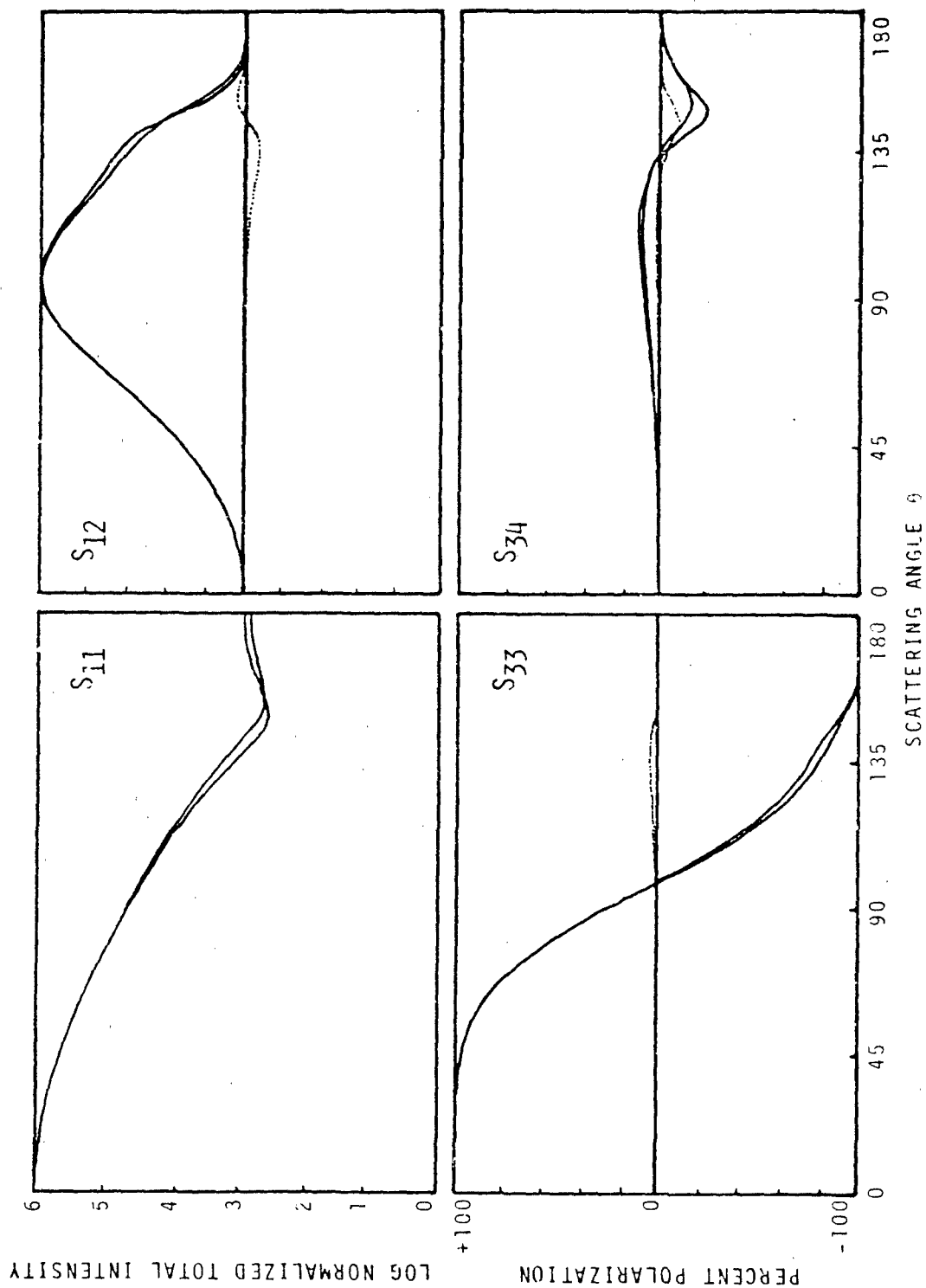
Figure 2. The Four Non-Zero Light Scattering Matrix Elements for 0.15 Micron Spheres Showing Their Response to a One Percent Increase in Radius (Solid Line) and Their Difference $\Delta = S_{ij}^L - S_{ij}^S$ (Dotted Line) $.4416\lambda$ $n_1 = 1.0$ $n_2 = 0$.
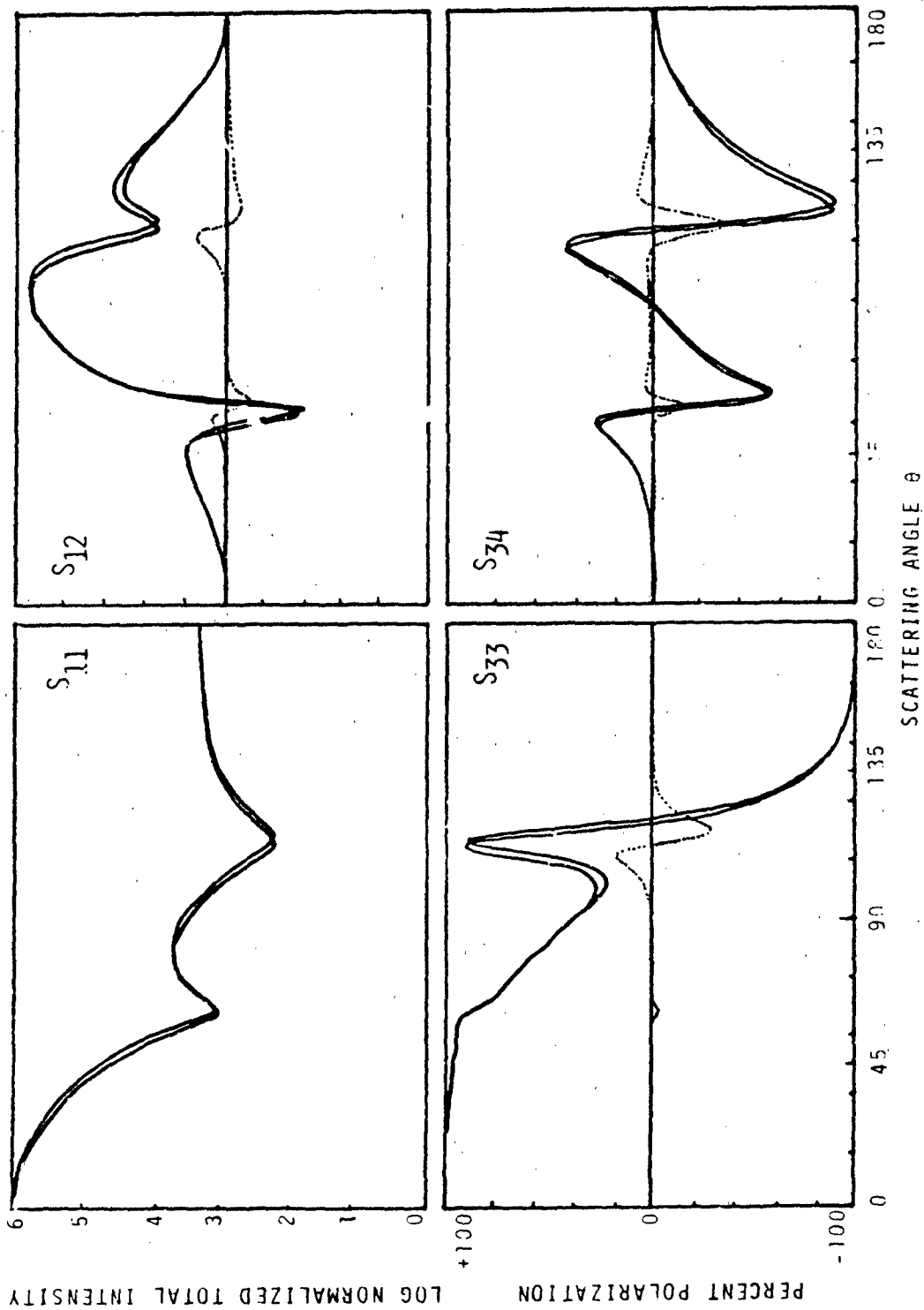
Figure 3. The Four Non-Zero Light Scattering Matrix Elements for 0.3 Micron Spheres Showing Their Response to a One Percent Increase in Radius (Solid Line) and Their Difference $\triangle = S_{ij}^L - S_{ij}^S$ (Dotted Line) $.4416\lambda$ $n_1 = 1.10$ $n_2 = 0$.
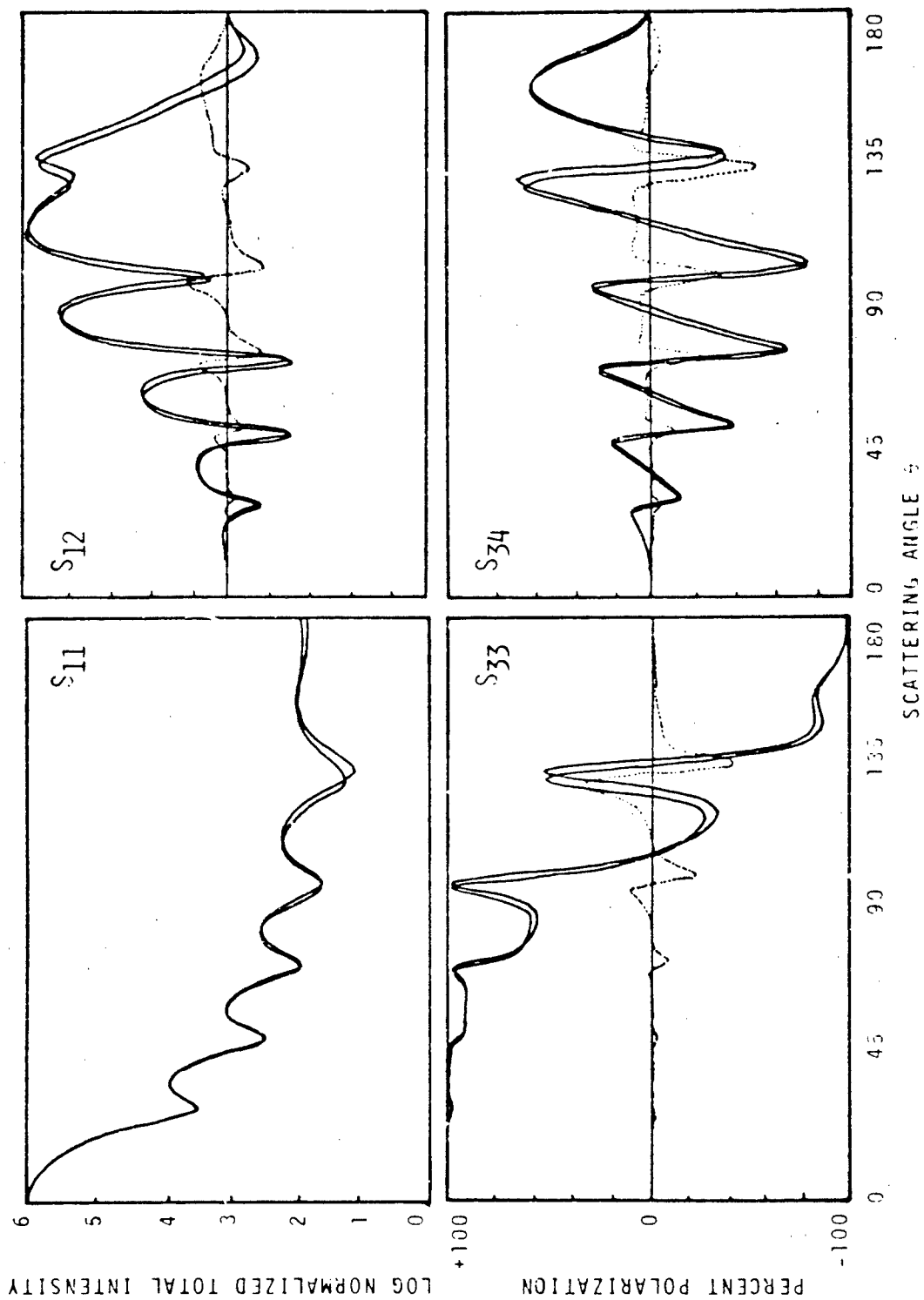
Figure 4. The Four Non-Zero Light Scattering Matrix Elements for 0.6 Micron Spheres Showing Their Responses to a One Percent Increase in Radius (Solid Line) and Their Difference $= S_{ij}^L - S_{ij}^S$ (Dotted Line). 4416A $n_1 = 1.10$ $n_2 = 0$.
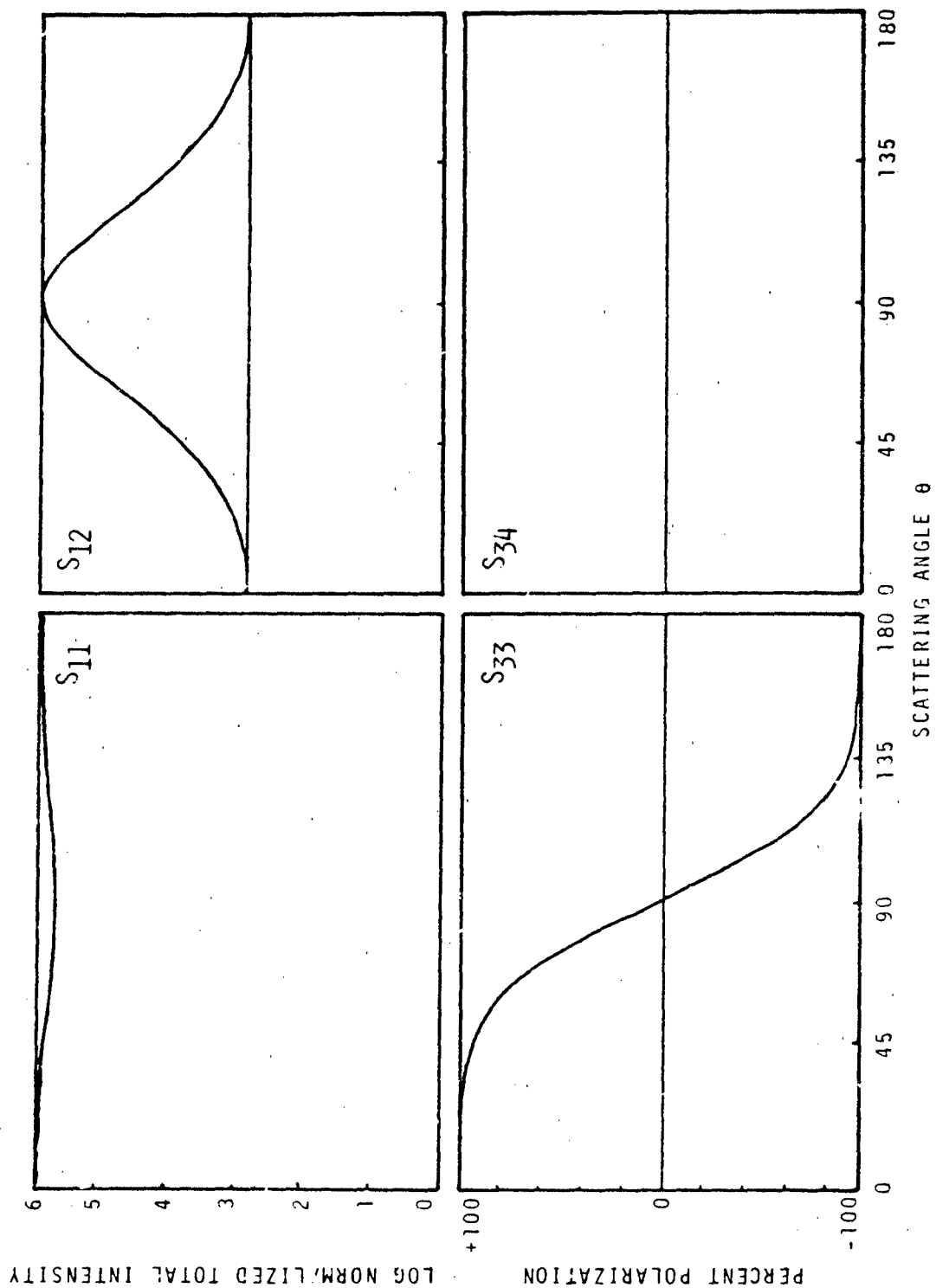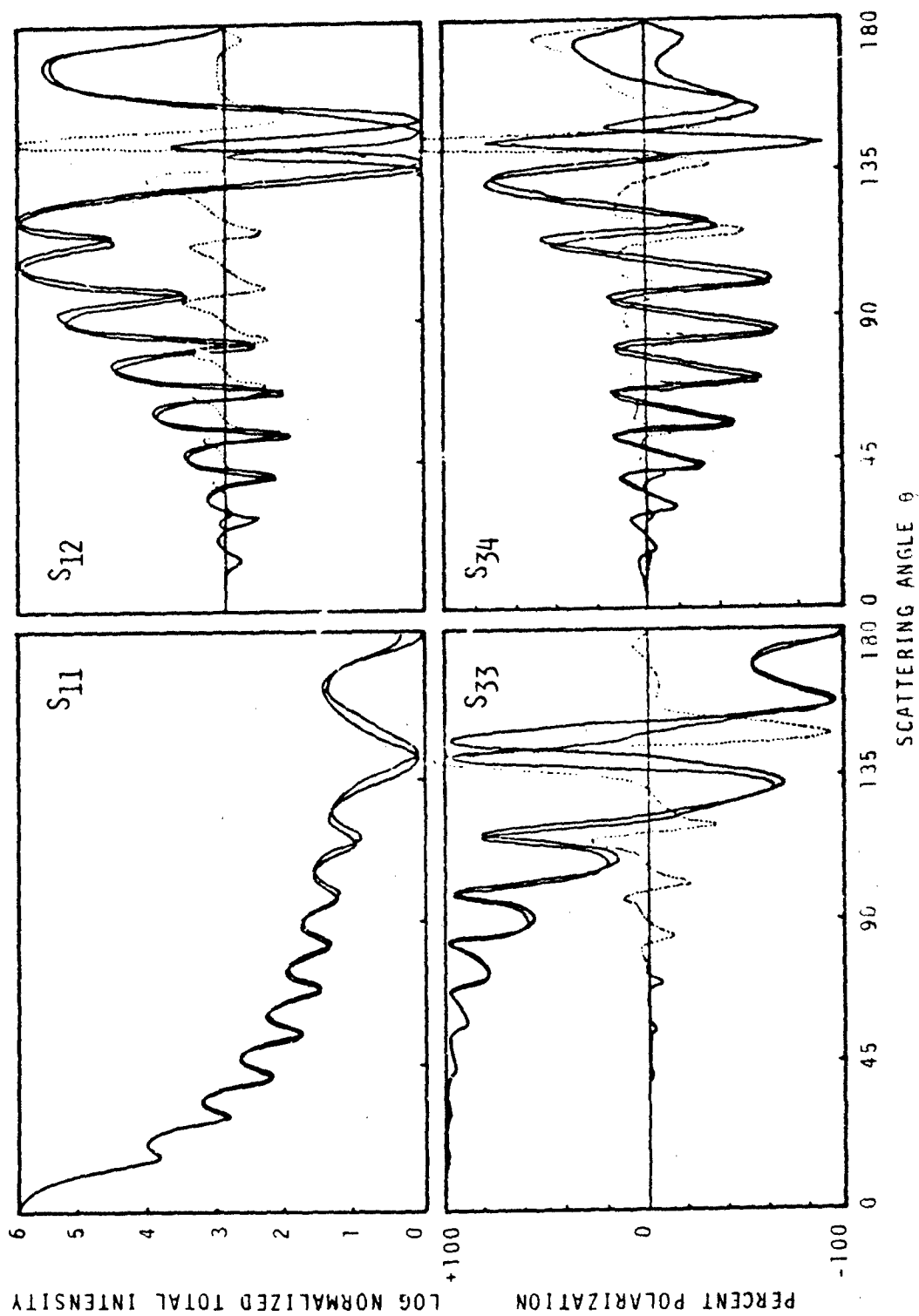
Figure 5. The Four Non-Zero Light Scattering Matrix Elements for 1.00 Micron Spheres Showing Their Response to a One Percent Increase in Radius (Solid Line) and Their Difference : = S_{ij}^L - S_{ij}^S (Dotted Line) .4416λ n_1 = 1.10 n_2 = 0.

1. Response to large size change.

Figure 1 shows the four non-zero matrix elements for a very small Rayleigh sphere ($r = 0.075\mu$). It can be solved exactly using the approximation that $r \ll \lambda$ yielding the three functions $\sin^2\theta$, $\cos\theta$ and zero for the matrix elements S_{12}, S_{33} and S_{34} respectively. Scanning each particular matrix element from Figure 1 to Figure 5 shows how each matrix element changes with increasing sphere radius. Increasing the radius approximately a factor of 2 going from Figure 1 to 5 causes all matrix elements to develop high frequency phase information. Each matrix element will be discussed individually.

Matrix element S_{11}

This matrix element represents the total intensity of light scattered by the particle. Unpolarized light illuminates the scatterer, and the total scattered intensity is measured. The vertical scale is logarithmetic, the curve has been normalized to maximum intensity at $\theta = 0$. As the particle increases size, S_{11} oscillates with increasing frequency. We also note that the ratio light scattered forward, ($\theta = 0$) to back ($\theta = 180^\circ$) increases. Larger particles scatter more light in the forward direction. For the particle studied here the ratio changes by 3 orders of magnitude. While this is generally true for low index particles, the ratio decreases as n_1 increases.

Matrix element S_{12}

This matrix element represents the extent to which the particle can distinguish between horizontally and vertically polarized light. If both were treated equally by the particle

S_{12} would be zero. As r increases, the initially smooth $\sin^2$ curve becomes distorted in the back scatter region, and finally developes oscillations about zero as large as $\pm 100\%$.

Matrix element S_{33}

This matrix element represents the extent to which the particle can distinguish between $+45^o$ and -45° polarization. If both were treated equally S_{33} would be zero. As r increases, the initally smooth cos curve becomes distorted and like S_{12} develops oscillations that can vary rapidly between $\pm 100\%$.

Matrix element S_{34}

This matrix element represents the extent to which the particle can distinguish between left-hand and right-hand circular polarization when illuminated with $+45^o$ or -45° linear polarization. If all combinations were treated equally S_{34} would be zero. As r increases, the initially zero S_{34} signal becomes non-zero and like the other S_{ij}, develops oscillations of increasing frequency and amplitude.

We can make the following observations about how the matrix elements respond to a large change in spherical particle size:

a. All matrix elements develop structure as the particle size increases. Quantifying the structure makes it possible to relate structure to particle size in some cases. For example in Figures 1-5 the number of maxima (or minima) in any matrix element curve is equal to the size of the particle in microns to within 10%. However, this is a special case and the results are fortuitously accurate for this combination of n_1, n_2 and r.

b. Large particles scatter more light into all angles than small particles. For the particles discussed here there is a 10^6

16

intensity difference between the small and large particle scatter-
ing efficiency.

c. The ratio (forward scatter:back scatter) increases as
the particle size increases. This is generally true for low
refractive index n_1. However as n_1 increases the ratio decreases
for constant r. Increasing absorption however increases the
ratio by removing more light from the backscatter.

d. Regardless of particle size, refractive index or absorp-
tion the following bounds govern all S_{ij} for spheres.

S_{11} initially decreases as θ increases from zero,

S_{12} is always zero at $\theta = 0$ and $\theta = 180^{\circ}$,

S_{33} is always +100% at $\theta = 0$ and -100% at $\theta = 180^{\circ}$,

S_{34} is always zero at $\theta = 0^{\circ}$ and $\theta = 180^{\circ}$

and zero everywhere for "very small" particles.

These bounds are obeyed even by mixtures of perfect spheres
polydispersed in n_1, n_2 and r. Fibers obey only the bound on S_{11}
and the bound that S_{34} is zero everywhere for "very small" fiber
radii.

e. Some special comments about S_{34}

The matrix element S_{34} has distinguished itself as a parti-
cularly important signature and sensitive probe of scattering
systems. Our initial experiments many years ago with biophysical
particles would have ended without success if S_{34} did not
uniquely survive to distinguish different polydispersed biologi-
cal particle systems. It is unfortunate that S_{34} is not as
experimentally accessable as the matrix elements S_{11} and S_{12}
which are responsible for most of the information obtained from

17

remote scattering systems. S_{34} is first a true indicator of "large particles" becoming non-zero as particle size goes from small to large (Rayleigh to Mie). For the system discussed here, S_{34} already shows a non-zero signal for r = 0.15µ, λ0.4416µ (n_1 = 1.10). Experimentally S_{34} is a powerful probe since large amplification of an initially zero S_{34} signal can yield a "full scale" reading for an arbitrarily small change in the signal. Thus the smallest deviation from zero will appear directly. This technique does not work for S_{12} and S_{33} which already have values of ±100 for small particles. For these elements, a small change must occur on an already large (full scale) signal. We have experimentally and theoretically investigated the ability of S_{12} and S_{33} to respond to a small increase in r by subtracting from them the "Rayleigh component", $S_{12} = \sin^2 \theta$ and $S_{33} = \cos^2 \theta$. The result, when amplified, can display approximately the same sensitivity as S_{34}. However, since noiseless signals do not occur experimentally, subtraction does not yield the same accuracy achieved from measuring S_{34} directly.

2. Response of S_{ij} to Small Size Change (Difference Curves).

Figures 1 through 5 which show the matrix elements for the five sphere sizes r = 0.075, 0.15, 0.30, 0.60 and 1.0 microns also show the matrix element signals that occur when the initial size is changed by a small value of 1%. Both matrix element curves are indicated by solid lines, and their difference $S^L_{ij} - S^S_{ij}$ is shown as a dotted line. We observe the following:

a. Figure 1. A 1% change in radius of a 0.075µ (Rayleigh) particle is not detected graphically at this level of sensiti-

18

vity. The actual numbers used to plot the curves show differences less than 0.1%, within the noise of most experiments.

b. <u>Figure</u> <u>2.</u> A 1% radius change in a 0.15μ particle changes all matrix elements. In addition, the difference occurs in the back scatter ($\theta \sim 90°$). S_{34} shows the largest difference, but is in competition with S_{12}.

c. <u>Figure</u> <u>3.</u> For larger particles (r = 0.3μ) changes occur both in forward and back scatter but are larger in the back scatter. Again S_{34} is most sensitive.

d. <u>Figure</u> <u>4.</u> A 1% change in even larger particles (r = 0.6μ) cause changes throughout the entire θ-range. Differences are larger in the back scatter and S_{34} is most sensitive.

e. <u>Figure</u> <u>5.</u> For our largest particles (r = 1.0μ), amplitude shifts caused by 1% size changes cause extremely large difference signals. Note that all difference curves go off the scale, $(S^L_{ij} - S^S_{ij}) > S_{ij}(max) = 100\%$ in the back scatter. S_{34} is most sensitive and the most sensitive region is $135° \leq \theta \leq 160°$.

f. <u>General</u> <u>Conclusions.</u>

Small changes (1%) in the radii of very small particles are not detected by any of the S_{ij}. Differences increase as particle size increases and appear in all S_{ij}. S_{34} is the most sensitive, giving the largest difference. All differences are larger in the back scatter. Phase shifts are not as dramatic as amplitude shifts. This is demonstrated by S_{34} in its response to a 1% change in a 1.0μ particle at $\theta = 145°$ (Figure 5).

All experimental and theoretical results discussed here are for perfect single spheres and fibers. Their implications become

19

very important for complex scattering systems such as _mixtures_ of

polydispersed perfect spheres, _irregular_ single particles or

mixtures of _irregular_ particles. The bounds on S_{ij} at $\theta = 0°$,

$90°$ and $180°$ discussed earlier will be violated on departure from

sphericity.

B. Arc Length as a Probe For Change.

Scanning each particular matrix element from Figures 1

through 5 shows how each matrix element responds to an increasing

sphere radius. The most obvious change in all signals is the

increasing frequency and amplitude of the oscillations. This

feature manifests itself as a change in arc length. We studied

the arc length of each S_{ij} as a function of particle radius and

obtained Figures 6 and 7.

The arc length is simply the geometrical length of the curve

in arbitrary units. A straight _horizontal_ line for all S_{ij} is

assigned an arc length of 180 (for $180°$). For S_{12}, S_{33} and S_{34} a

straight horizontal line starting at $\theta = 0$, $\pi = 0\%$ going to

$\theta = 0$, $\pi = 100\%$; to $\theta = 180°$ $\pi = 100\%$; and then to $\theta = 180°$ $\pi = 0\%$

has an arc length of $(100 + 180 + 100) = 380$ units. The same

geometrical value occurs for the normalized S_{11} curves. Arc

length becomes valuable when different curves or families of

curves are compared.

Figure 6 shows two useful results:

1. Arc lengths of S_{12}, S_{33} and S_{34} increase more or less

monotonically with increasing radius.

2. The arc lengths of S_{11} oscillate wildly and are not

monotonic.
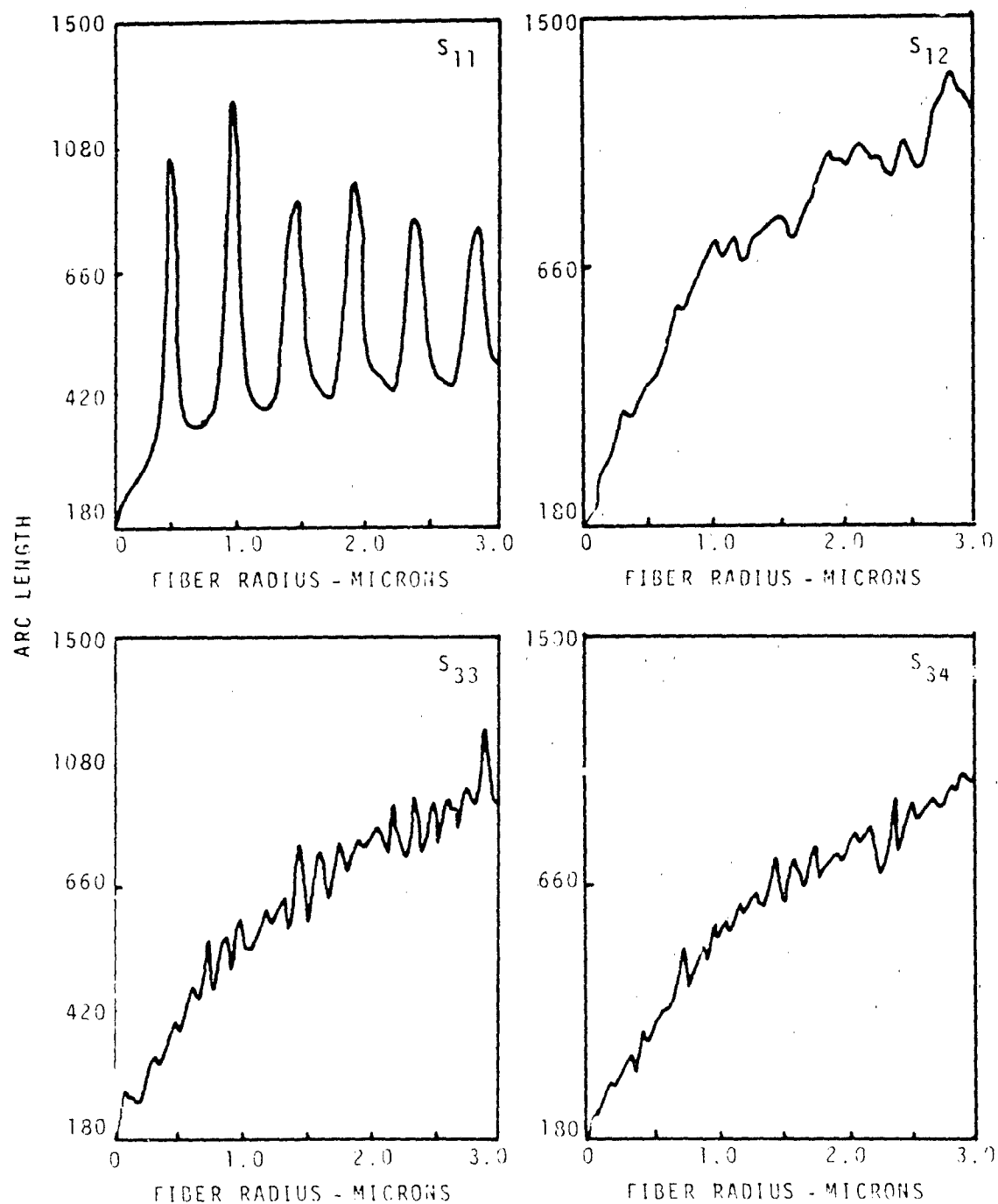
ARC LENGTH

Figure 6.   The Arc Length of Four Matrix Elements as a Function
of Fiber Radius for n_1 = 1.4662, n_2 = 0.0 and λ = 0.4416 Microns.

21

Figure 7. The Arc Length, Area Under the Curve and Extinction Coefficient Determined from S_{11} as a Function of Fiber Radius for $n_1 = 1.4662$, $n_2 = 0.0$ and $\lambda = 0.4416$ Microns.

The arc length of S_{11} is not an accurate probe for changing particle size. For a particular radii (close to $r = 1.0\mu$) the arc length could decrease by more than a factor of 3 for a 30% increase or decrease in size. The other S_{ij} possess some structure but give more accurate results. The relationship between radius r and arc length AL of S_{33} and S_{34} is given by

$$r(\text{microns}) \doteq \sqrt{\frac{AL-180}{113.2}}$$

Note that for larger particles ($r > 1.5\mu$) the AL of S_{12} is larger than that of S_{33} and S_{34}. For smaller particles ($r < 1.0\mu$) the relationship is

$$r(\text{microns}) \doteq \frac{(AL-180)}{45}$$

Although it is well-known that certain features of S_{ij} curves change with particle property, previously, only limited attention has been given to quantifing the change as we are doing here. These observations are important for monitoring changes that occur in system parameters during time resolved or biological experiments, for example, where often the exact optical properties are not as important as knowing what changed and by how much.

Further study of S_{11} arc length led to some interesting results. We noticed that the arc length oscillations in S_{11} are similar to the well-known cross section oscillations that occur as a function of particle radius. More fundamental than the arc length however is the area under S_{11} which represents the total energy scattered by the particle. This line of reasoning led to

23

Figure 7 which shows how the arc length compares to the area under S_{11} which when multiplied by $\frac{4}{3}\pi r^3$ yields the well-known extinction coefficient as a function of r. Therefore arc length of S_{11} has a behavior similar to the fundamental particle property--the extinction cross section. The other S_{ij} arc lengths are not fundamental but useful nevertheless as probes for changes in particle parameters.

Results of similar arc length data as a function of n_1 and n_2 will be published.

C. Fourier Transforms as a Probe For Change.

The increasing oscillatory structure on S_{ij} curves resulting from increasing radius has been shown in Figures 1-5. The S_{ij} curves are expansions of integral order Bessel functions whose amplitudes are varied by harmonic functions. Our studies of the Fourier transforms of the S_{ij} give additional information about the scatterer and the relative sensitivity of various S_{ij} to particle parameter change. Figures 8, 9 and 10 show the FT three sets of particles respectively: r = 0.25μ and 0.30μ; r = 0.55μ and 0.60μ; and r = 2.5μ and 2.6μ. We observe the following:

1. Increasing particle size introduces more oscillatory structure (higher frequency components) on all S_{ij}.

2. S_{11} has a low frequency continuum lacking significant monochromatic features.

3. S_{33} is only slightly better than S_{11} possessing a low frequency continuum (initially it is $\cos^2\theta$) and a few quantized frequency components for larger particles.

4. S_{12} and S_{34} are very competitive. They both display
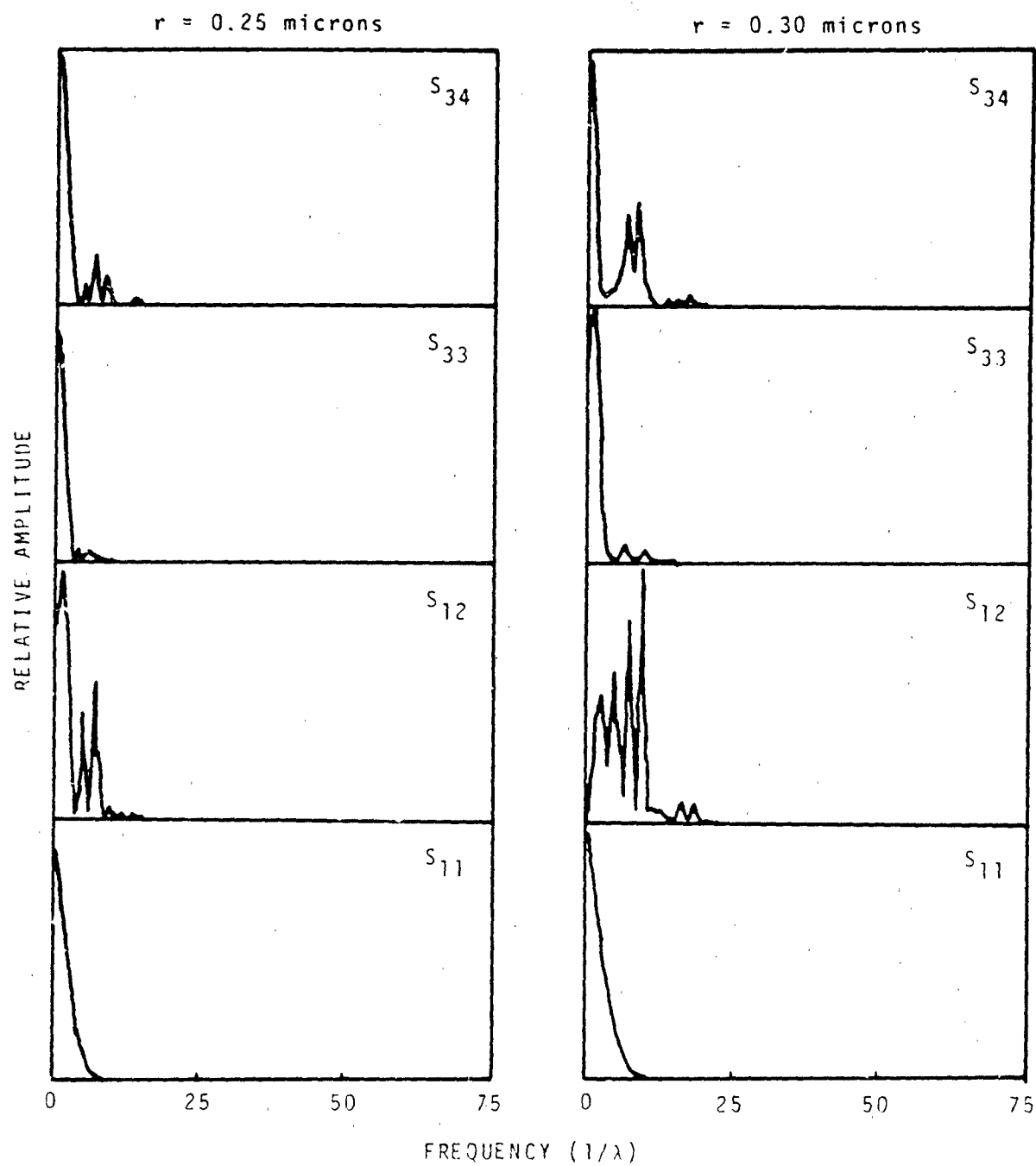
Figure 8. Amplitude-Frequency Distributions of Four Non-Zero
Fiber Matrix Elements and Their Response to a Small Change in the
Radius of a 0.25 Micron Fiber. $\lambda 4416\text{Å}$ $n_1 = 1.466$ $n_2 = 0$.

25
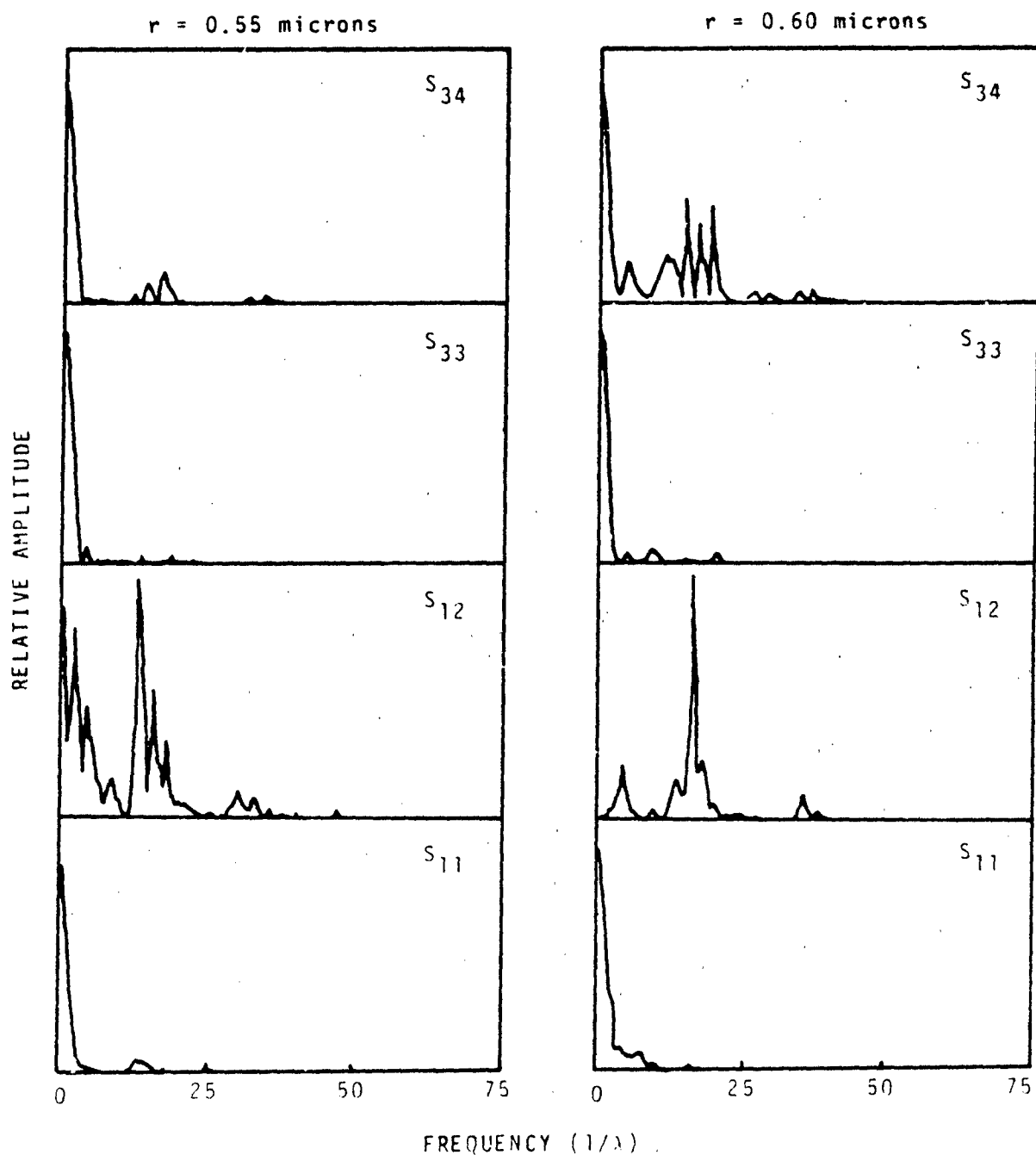
Figure 9.   Amplitude-Frequency Distributions of Four Non-Zero

Fiber Matrix Elements and Their Response to a Small Change in the

Radius of a 0.55 Micron Fiber.   4416Å n_1 = 1.466 n_2 = 0.
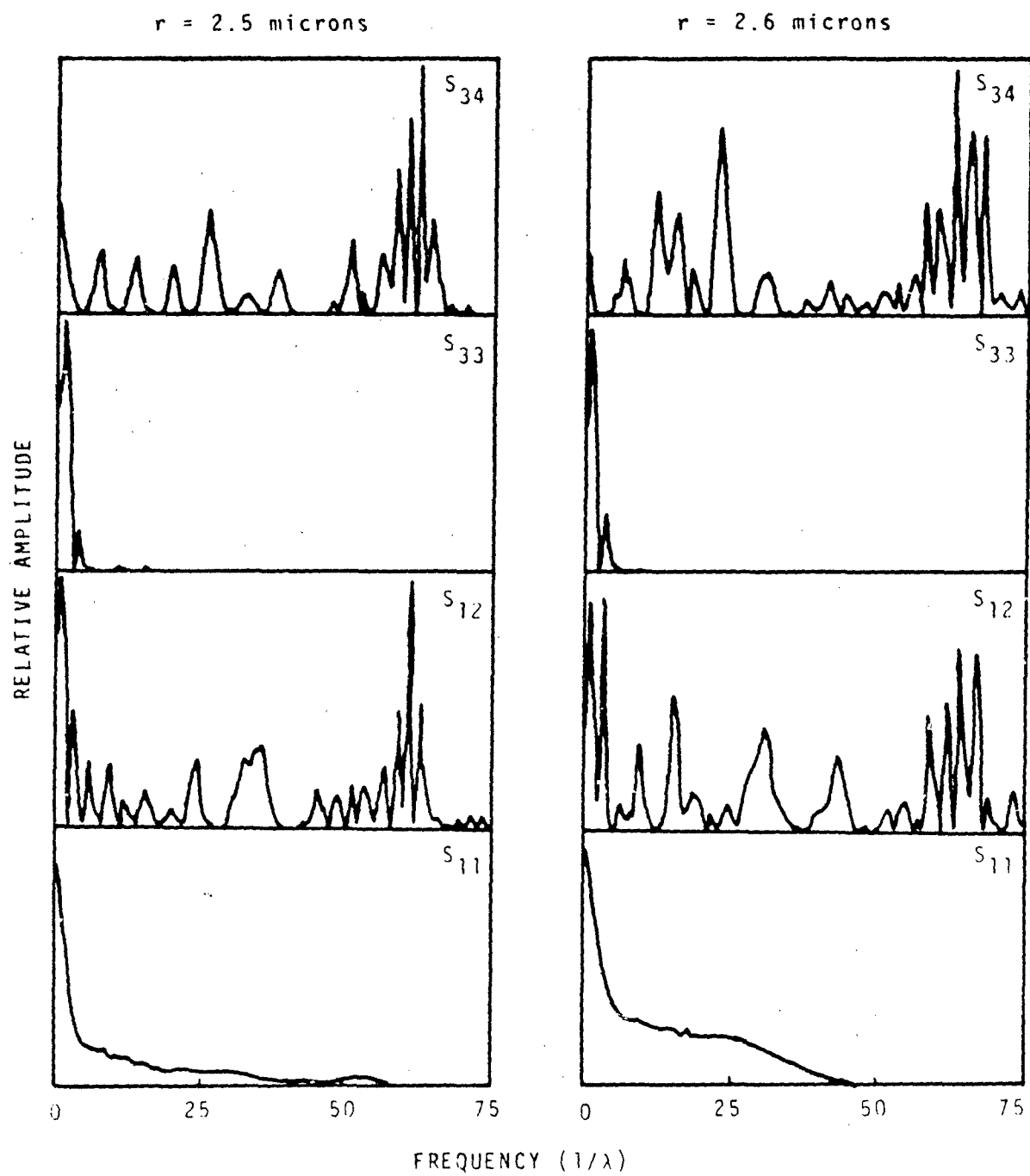
Figure 10. Amplitude-Frequency Distributions of Four Non-Zero
Fiber Matrix Elements and Their Response to a Small Change in the
Radius of a 2.5 Micron Fiber. $\lambda 4416A$ $n_1 = 1.466$ $n_2 = 0$.

27

extensive quantized frequency information for the same size

particle and also compete as a detector of small size change.

However S_{34} might be more reliable since the number of components

increase as r increases whereas the number of components in S_{12}

remain constant or change only slightly. When components and

amplitudes are taken into account, S_{12} and S_{34} are comparable and

serve well as signatures and indicators of change. S_{12} is more

readily accessible to remote sensing experiments since it couples

unpolarized (total intensity) incident on the scatterer with

horizontally polarized scattered light.

It is interesting to observe the relative efficiency of

representing the S_{ij} in terms of Bessel functions as compared to

Fourier transforms - both of which make a complete mathematical set.

To generate a particular set of S_{ij} requires about twice to three

times as many Fourier coefficients as Bessel coefficients. This

is due to the natural cylindrical geometry of the scattering

system which lends itself directly to Bessel's equation and a

Bessel function solution.

D.   Information Contained in Forward and Back Scatter

We investigated the amount of information contained in

the forward scattered and back scattered light into small θ near

$\theta = 0$ and $\theta = 180^o$, respectively. This satisfies objective E. Many

ground based remote sensing experiments have access only to back

scatter information from light scattered back to the laser site.

Figure 11 shows the intensities of forward ($\theta = 0^o$) and back

scattered ($\theta = 180^o$) light as a function of sphere radius for

spheres with various optical constants. Figure 11 can be studied

in several ways.

28
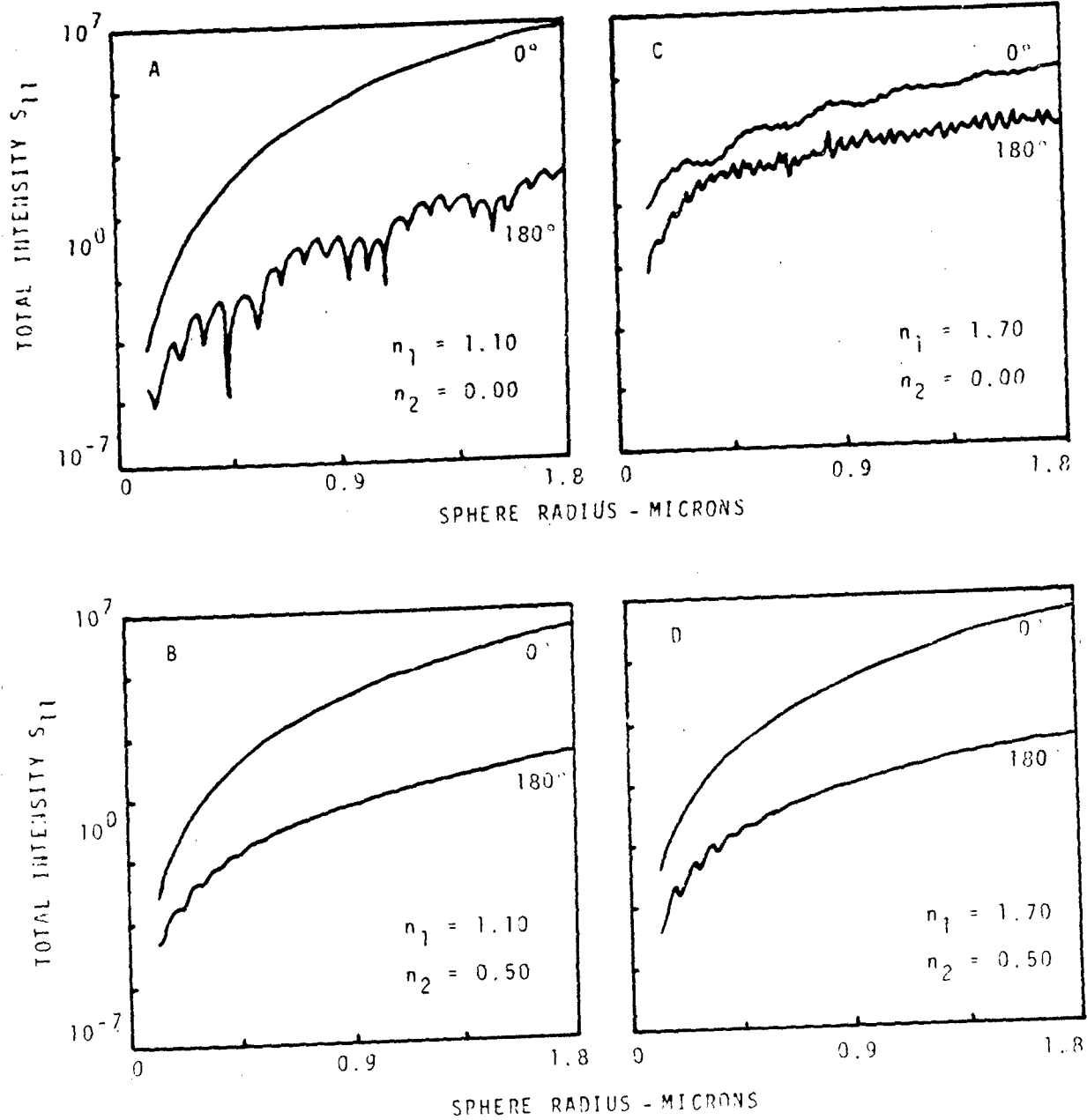
Figure 11. Forward Scatter ($\theta = 0$) and Back Scatter ($\theta = 180°$) Efficiencies as a Function of Sphere Radius and Optical Constants.

Change n_1 from 1.1 to 1.7 with n_2 = 0 go from A to C.

Change n_1 from 1.1 to 1.7 with n_2 = 0.5 go from B to D.

Change n_2 from 0 to 0.5 with n_1 = 1.1 go from A to B.

Change n_2 from 0 to 0.5 with n_1 = 1.7 go from C to D.

   a. <u>Figure 11-A.</u> The forward scatter (θ = 0) from particles of small n_1 (n_1 = 1.1) and n_2 (n_2 = 0.0) increases smoothly and monotonically over 10 orders of magnitude for a one order of magnitude increase in radius. This says that one 1.5μ particle scatters, the the forward direction, as much light as 10^{10} 0.15μ particles. This is an effective way to hide particles or particle information.

   The back scatter (θ = 180°) increases also, but only by 7 orders of magnitude. In addition it is not monotonic. For example, <u>increasing</u> or <u>decreasing</u> the size of a 0.45 particle <u>increases</u> the scattered intensity by 3 orders of magnitude making the back scatter intensity information non-unique to particle size. Back scatter measurements are very sensitive to particle change, but not good indicators of particle size. They are good <u>probes</u> but not good <u>signatures</u>.

   b. <u>Figure 11-B.</u> Absorption (n_2 = 0.5) destroys virtually all structure in the back scatter. Both forward and back scatter curves are essentially monotonic. However, the intensity ratio: forward to back scatter, remains about the same as that for particles with zero absorption (n_2 = 0) shown in Fig. A.

   c. <u>Figure 11-C.</u> The intensity of both forward and back scattered light from large index particles (n_1 = 1.7) with no absorption (n_2 = 0) oscillates with increasing particle size.

3The forward scatter oscillations are larger, the back scatter oscillations are smaller for larger n_1. In addition, the ratio of forward to back scatter remains essentially constant ($\sim 10^2$), independent of particle size.

d. _Figure 11-D._ Scattering from high index ($n_1 = 1.7$) and high absorption ($n_2 = 0.5$) spheres displays oscillations in the back scatter only for smaller particles ($r < 0.7\mu$).

e. General Conclusions

Low refractive index spheres scatter light in the _forward_ direction with an intensity that increases smoothly and monotonically with increasing particle size – essentially independent of the amount of absorption. Absorption destroys oscillation in both the forward and back scatter – essentially independent of the value of n_1.

Back scatter information is a sensitive probe for change but not a unique indicator of size. Back scatter information that does not oscillate with wavelength must come from particles with large absorption (assuming that n_2 stays large over the θ-range). Conversely substantial θ-dependent oscillation in the back scatter must be caused by low absorption and low index particles. In general, there is more information in back scatter than in forward scatter – which is fortunate for many ground based remote sensing experiments.

All observations discussed above are valid for single spheres or monodispersed sphere systems. Polydispersity and/or systems of irregular particles will destroy phase-amplitude information. Exactly what information remains is the subject of our present research.

31

E. Average, mean or effective refractive index

This study satisfies research objective D and has been published in Aerosol Science and Technology 1:329-335(1982).

F. Stokes Vectors, Mueller Matrices and polarized light scattering

This study satisfies research objective F. A paper has been submitted to the American Journal of Physics.

III. FINAL COMMENTS

This final report describes the main thrust of our research and a number of experimental results from which conclusions were drawn to make our point concerning the information contained in the matrix elements. At best, significant trends can be established. To investigate all combinations of r, n_1 and n_2 would yield an infinitely large data bank too unwieldy to analyze. We attempted to limit our particles into regions: size-large, medium, small; refractive index and absorption-high, medium, low and chose carefully combinations that will establish a trend or generate an exception. This approach has been productive and has given good insight to the information contained in light scattering data.

APPENDIX A

COLLOQUIA, SEMINARS AND CONFERENCES

Conferences: 1. CSL on light scattering, Aberdeen, Maryland, June 15-17, 1981.

2. Conference on Aerosol Science, Santa Monica, California, February 20-23, 1982.

Colloquia: 1. Optical Sciences Department, University of Arizona, Spring 1982.

2. SERI, Golden, Colorado, Summer 1981.

3. Physics Department, University of Lund, Lund, Sweden, Summer 1982.

4. Physics Department, University of Arizona, Fall 1982.

Seminars: 1. SERI, Golden, Colorado, Summer 1981.

2. Physics Department, University of Lund, Lund, Sweden, Summer 1982.

BLANK

APPENDIX B

PAPERS

1. "Masking of Information in Light Scattering Signals from Complex Scatterers", William S. Bickel, Hashim A. Yousif and Wilbur M. Bailey, Aerosol Science and Technology 1:329-335 (1982).

2. "Light Scattering from Fibers - an Extension of a Single Slit Diffraction Experiment", Wolfgang Gilliar and William S. Bickel, submitted to Am. J. of Physics.

3. "The Physical and Optical Properties of Agglomerated Gold Films Optical Scattering from Surfaces", Richard Zito, William S. Bickel and Wilbur M. Bailey, submitted to Applied Optics.

4. "Stokes Vectors, Mueller Matrices and Polarized Scattered Light", William S. Bickel and Wilbur M. Bailey, submitted to Am. J. Physics.

5. "Light Diffraction Studies of Single Muscle Fiber as a Function of Fiber Rotation", Wolfgang Gilliar and William S. Bickel, accepted by Biophysical Journal.

6. "Light Scattering from Geometrically Perturbed Thin Fiber," William S. Bickel and Gordon Videen, to be submitted to App. Optics.

7. "Information Content in LS Signals from Mixtures, Polytidpersed and Multiple Scattering System", William S. Bickel, Wilbur M. Bailey and Hashim A. Yousif, to be submitted to Applied Optics.

8. "Sensitivity of LS Matrix Elements to Small Changes in Structural and Optical Constants of Perfect Scatterers", William S. Bickel, W. M. Bailey and H. A. Yousif, _to be submitted_ to Aerosol Science and Technology.

9. "Scattering Corrections to ORD and CD Measurements", William S. Bickel, to be submitted to App. Optics.

DISTRIBUTION LIST FOR ARDC-CR-83027

Names	Copies	Names	Copies
CHEMICAL SYSTEMS LABORATORY			
		Defense Advanced Research Projects Agency	
ATTN: DRSMC-CLB (A)	1	ATTN: Dr. Tegnella	1
ATTN: DRSMC-CLB-C (A)	1	Washington, DC 20301	
ATTN: DRSMC-CLB-P (A)	1		
ATTN: DRSMC-CLB-PS (A)	4	Office of the Director	
ATTN: DRSMC-CLB-R (A)	1	Defense Research and Engineering	
ATTN: DRSMC-CLB-T (A)	1	ATTN: Dr. T.C. Walsh, Rm 3D-1079	1
ATTN: DRSMC-CLB-TE (A)	1	Washington, DC 20310	
ATTN: DRSMC-CLC-B (A)	1		
ATTN: DRSMC-CLC-C (A)	1	Advanced Research Projects Agency	1
ATTN: DRSMC-CLF (A)	1	1400 Wilson Boulevard	
ATTN: DRSMC-CLJ-IL (A)	2	Arlington, VA 22209	
ATTN: DRSMC-CLJ-IR (A)	1		
ATTN: DRSMC-CLJ-M (A)	1	DEPARTMENT OF THE ARMY	
ATTN: DRSMC-CLJ-P (A)	1		
ATTN: DRSMC-CLN (A)	1	HQDA	
ATTN: DRSMC-CLN-S (A)	1	ATTN: DAMO-NCC	1
ATTN: DRSMC-CLN-ST (A)	1	ATTN: DAMA-ARZ (Dr. Verdorame)	1
ATTN: DRSMC-CLR-I (A)	1	ATTN: DAMI-FIT	1
ATTN: DRSMC-CLT (A)	1	WASH DC 20310	
ATTN: DRSMC-CLW-C (A)	1		
ATTN: DRSMC-CLY-A (A)	1	HQDA	
ATTN: DRSMC-CLR-I (A)	1	Office of the Deputy Chief of Staff for	
ATTN: DRSMC-CLY-R (A)	1	Research, Development & Acquisition	
		ATTN: DAMA-CSS-C	1
COPIES FOR AUTHOR(S)		Washington, DC 20310	
DRSMC-CLB-PS (A)	26		
RECORD COPY: DRSMC-CLB-A (A)	1	HQ Sixth US Army	
		ATTN: AFKC-OP-NBC	1
DEPARTMENT OF DEFENSE		Presidio of San Francisco, CA 94129	
Defense Technical Information Center		Commander	
ATTN: DTIC-DDA-2	12	DARCOM, STITEUR	
Cameron Station, Building 5		ATTN: DRXST-STI	1
Alexandria, VA 22314		Box 48, APO New York 09710	
Director		Commander	
Defense Intelligence Agency		USASTCFEO	
ATTN: DB-4G1	1	ATTN: MAJ Mikeworth	1
Washington, DC 20301		APO San Francisco 96328	
Deputy Under Secretary of Defense for		HQ, 5th Infantry Div	
Research and Engineering (R&AT)		ATTN: Div Cml Off	1
ATTN: Dr. Musa	1	Ft Polk, VA 71459	
ATTN: COL Friday	1		
ATTN: COL Winter	1		
ATTN: Mr. Thomas Dashiell	1		
Washington, DC 20301			

Army Research Office
ATTN: DRXRO-CB (Dr. R. Ghirardelli)   1
ATTN: DRXRO-GS   1
ATTN: Dr. W. A. Flood   1
P.O. Box 12211
Research Triangle Park, NC   27709

HQDA ODUSA (OR)   1
ATTN: Dr. H. Fallin
Washington, DC   20310

HQDA (DAMO-FDD)   1
ATTN: MAJ C. Collat
Washington, DC   20310

HQDA, OCE   1
ATTN: DAEN-RDM (Dr. Gomez)
Massachusetts Ave, NW
Washington, DC   20314

Commander   1
89th Medical Group (P)
3135 George Washington Blvd
Wichita, KS   67210

OFFICE OF THE SURGEON GENERAL

Commander
US Army Medical Research and
     Development Command
ATTN: SGRD-UBD-AL (Bldg 568)   1
ATTN: SGRD-UBG (Mr. Eaton)   1
ATTN: SGRD-UBG-OT (CPT Johnson)   1
ATTN: LTC Don Gensler   1
Fort Detrick, MD   21701

Commander
US Army Medical Bioengineering Research
     and Development Laboratory
ATTN: SGRD-UBD-AL, Bldg 568   1
Fort Detrick, Frederick, MD   21701

Commander
USA Medical Research Institute of
     Chemical Defense
ATTN: SGRD-UV-L   1
Aberdeen Proving Ground, MD   21010

US ARMY MATERIEL DEVELOPMENT AND
     READINESS COMMAND

Commander
HQ, DARCOM
ATTN: DRCED (BG Robinson)   1
5001 Eisenhower Ave.
Alexandria, VA   22333

Commander
US Army Materiel Development and
     Readiness Command
ATTN: DRCDE-DM   1
ATTN: DRCMT   1
ATTN: DRCSF-P   1
ATTN: DRCSF-S   1
ATTN: DRCDL (Mr. N. Klein)   1
ATTN: DRCDMD-ST (Mr. T. Shirata)   1
5001 Eisenhower Ave
Alexandria, VA   22333

Commander
US Army Foreign Science & Technology Center
ATTN: DRXST-MT3   1
ATTN: DRXST-MT3 (Poleski)   1
220 Seventh St., NE
Charlottesville, VA   22901

Director
Human Engineering Laboratory
ATTN: DRXHE-IS   1
Aberdeen Proving Ground, MD   21005

Commander
US Army Natick Research and
     Development Laboratories
ATTN: DRDNA-ITF (Dr. Roy W. Roth)   1
Natick, MA   01760

Director
DARCOM Field Safety Activity
ATTN: DRXOS-SE (Mr. Yutmeyer)   1
Charlestown, IN   47111

PM Smoke/Obscurants
ATTN: DRCPM-SMK-E (A. Van de Wal)   1
ATTN: DRCPM-SMK-M   1
ATTN: DRCPM-SMK-T   1
Aberdeen Proving Ground, MD   21005

Director
US Army Materiel Systems Analysis Activity
ATTN: DRXSY-MP   1
ATTN: DRXSY-CR (Mr. Metz)   1
ATTN: DRXSY-FJ (J. O'Bryon)   1
ATTN: DRXSY-GP (Mr. Fred Campbell)   1
Aberdeen Proving Ground, MD   21005

USA AVIATION RESEARCH AND
    DEVELOPMENT COMMAND

Director
Applied Technology Lab
USARTL (AVRADCOM)
ATTN: DAVDL-ATL-ASV   1
ATTN: DAVDL-ATL-ASW   1
ATTN: DAVDL-EV-MOS (Mr. Gilbert)   1
Ft. Eustis, VA   23604

Commander
USA Avionics R&D Activity
ATTN: DAVAA-E (M. E. Sonatag)   1
Ft. Monmouth, NJ   07703

USA MISSILE COMMAND

Commander
US Army Missile Command
Director, Energy Directorate
ATTN: DRSMI-RHFT   1
ATTN: DRSMI-RMST   1
ATTN: DRSMI-YLA (N. C. Katos)   1
Redstone Arsenal, AL   35809

Commander
US Army Missile Command
Redstone Scientific Information Center
ATTN: DRSHI-REO (Mr. Widenhofer)   1
ATTN: DRSMI-RGT (Mr. Matt Maddix)   1
ATTN: DRSMI-RKL (Dr. W. Wharton)   1
ATTN: DRDMI-CGA (Dr. B. Fowler)   1
ATTN: DRDMI-TE (Mr. H. Anderson)   1
Redstone Arsenal, AL   35809

Commander
US Army Missile Command
Redstone Scientific Information Center
ATTN: DRSMI-RPR (Documents)   1
Redstone Arsenal, AL   35809

USA COMMUNICATIONS-ELECTRONICS COMMAND

Commander
USA Communications-Electronics Command
ATTN: DRSEL-WL-S (Mr. J. Charlton)   1
Ft. Monmouth, NJ   07703

Commander
USA Electronics Research and
    Development Command
ATTN: DRDEL-CCM (Dr. J. Scales)   1
ATTN: DELHD-RT-CB (Dr. Sztankay)   1
Adelphi, MD   20783

Commander
Harry Diamond Laboratories
ATTN: DRXDO-RCB (Dr. Donald Wortman)   1
ATTN: DRXDO-RCB (Dr. Clyde Morrison)   1
ATTN: DRXDO-RDC (Mr. D. Giglio)   1
2800 Powder Mill Road
Adelphi, MD   20783

Commander
USA Materials & Mechanics Research Center
ATTN: DRXMR-KA (Dr. Saul Isserow)   1
Watertown, MA   02172

Commander
USA Cold Region Research Engineering Laboratory
ATTN: George Aitken   1
Hanover, NH   03755

Commander/Director
Combat Surveillance and Target
    Acquisition Laboratory
ERADCOM
ATTN: DELCS-R (E. Frost)   1
Ft. Monmouth, NJ   07703

Director
Atmospheric Sciences Laboratory
ATTN: DELAS-AR (H. Holt)   1
ATTN: DELAS-AS (Dr. Charles Bruce)   1
ATTN: DELAS-AS-P (Mr. Tom Pries)   1
ATTN: DELAS-EO-EN (Dr. Donald Snider)   1
ATTN: DELAS-EO-EN (Mr. James Gillespie)   1
ATTN: DELAS-EO-ME (Dr. Frank Niles)   1
ATTN: DELAS-EO-ME (Dr. Ronald Pinnick)   1
ATTN: DELAS-EO-MO (Dr. Melvin Heaps)   1
ATTN: DELAS-EO-MO (Dr. R. Sutherland)   1
ATTN: DELAS-EO-S (Dr. Louis Duncan)   1
White Sands Missile Range, NM   88002

US ARMY ARMAMENT, MUNITIONS AND
    CHEMICAL COMMAND

Commander
US Army Armament, Munitions and
    Chemical Command
ATTN: DRSMC-ASN (R)   1
ATTN: DRSMC-IRI-A (R)   1
ATTN: DRSMC-LEP-L (R)   1
ATTN: DRSMC-SF (R)   1
Rock Island, IL 61299

Commander
US Army Dugway Proving Ground
ATTN: Technical Library (Docu Sect)   1
Dugway, UT 84022

US ARMY ARMAMENT RESEARCH AND
    DEVELOPMENT CENTER

Commanding Officer
Armament Research and Development Center
USA AMCCOM
ATTN: DRSMC-LCA-L (D)   1
ATTN: DRSMC-LCE (D) (Mr. Scott Morrow) 1
ATTN: DRSMC-LCE-C (D)   1
ATTN: DRSMC-LCU-CE (D)   1
ATTN: DRSMC-SCA-T (D)   1
ATTN: DRSMC-SCF (D)   1
ATTN: DRSMC-SCP (D)   1
ATTN: DRSMC-SCS (D)   1
ATTN: DRSMC-TDC (D) (Dr. D. Gyorog)   1
ATTN: DRSMC-TSS (D)   2
ATTN: DRCPM-CAWS-AM (D)   1
Dover, NJ 07801

Armament Research and Development Center
USA AMCCOM
ATTN: DRSMC-TSE-OA (Robert Thresher) 1
National Space Technology Laboratories
NSTL Station, MS 39529

Requirements and Analysis Office
Foreign Intelligence and Threat
    Projection Division
ATTN: DRSMC-RAI-C (A)   1
Aberdeen Proving Ground, MD 21010

Commanding Officer
Armament Research and Development Center
USA AMCCOM
ATTN: DRSMC-QAC-O (A) (Mr. Francis)   1
ATTN: DRSMC-QAC-E (A)   1
Aberdeen Proving Ground, MD 21010

Commanding Officer
Armament Research and Development Center (BRL)
USA AMCCOM
ATTN: DRSMC-BLB (A)   1
ATTN: DRSMC-TSB-S (A)   1
Aberdeen Proving Ground, MD 21005

US ARMY TRAINING & DOCTRINE COMMAND

Commandant
US Army Infantry School
ATTN: CTDD, CSD, NBC Branch   1
Fort Benning, GA 31905

Commandant
US Army Missile & Munitions Center
    and School
ATTN: ATSK-CM   1
Redstone Arsenal, AL 35809

Commander
US Army Logistics Center
ATTN: ATCL-MG   1
Fort Lee, VA 23801

Commandant
US Army Chemical School
ATTN: ATZN-CM-C   1
ATTN: ATZN-CM-AFL   2
ATTN: ATZN-CN-CDM (Dr. J. Scully)   1
ATTN: Combat Dev Smoke (CPT Gray)   1
Fort McClellan, AL 36205

Commander
USAAVNC
ATTN: ATZC-D-MS   1
Fort Rucker, AL 36362

Commander
USA Combined Arms Center and
    Fort Leavenworth
ATTN: ATZL-CAM-IM   1
Fort Leavenworth, KS 66027

Commander
US Army Infantry Center
ATTN: ATSH-CD-MS-C   1
ATTN: ATSH-CD-MS-F   1
ATTN: ATZB-OPT-PO-NBC   1
Fort Benning, GA 31905

Commander
USA Training and Doctrine Command
ATTN: ATCD-N   1
ATTN: ATCD-TEC (Dr. M. Pastel)   1
ATTN: ATCD-Z   1
Fort Monroe, VA   23651

Commander
US Army Armor Center
ATTN: ATZK-CD-MS   1
ATTN: ATZK-PPT-PO-C   1
Fort Knox, KY   40121

Commander
US Army TRADOC System Analysis Activity
ATTN: ATAA-SL   1
ATTN: ATAA-TDB (L. Dominguez)   1
White Sands Missile Range, NM   88002

Commander
USA Field Artillery School
ATTN: ATSF-GD-RA   1
Ft. Sill, OK   73503

Director
USA Concepts Analysis Agency
ATTN: MOCA-SMC (Hal Hock)   1
8120 Woodmont Avenue
Bethesda, MD   20014

US ARMY TEST & EVALUATION COMMAND

Commander
US Army Test & Evaluation Command
ATTN: DRSTE-CM-F   1
ATTN: DRSTE-CT-T   1
ATTN: ORSTE-AO-M (Warren Baity)   1
Aberdeen Proving Ground, MD   21005

Commander
USA EPG
ATTN: STEEP-MM-IS   1
ATTN: STEEP-MT-DS (CPT Decker)   1
Ft. Huachuca, AZ   85613

Commander
Dugway Proving Ground
ATTN: STEDP-MT (Dr. L. Solomon)   1
Dugway, UT   34022

DEPARTMENT OF THE NAVY

Commander
Naval Research Laboratory
ATTN: Code 5709 (Mr. W. E. Howell)   1
ATTN: Code 6532 (Mr. Curcio)   1
ATTN: Code 6532 (Mr. Trusty)   1
ATTN: Code 6530-2 (Mr. Gordon Stamm)   1
ATTN: Code 8320 (Dr. Lothar Ruhnke)   1
ATTN: Code 8326 (Dr. James Fitzgerald)   1
ATTN: Code 43202 (Dr. Hermann Gerber)   1
4555 Overlook Avenue, SW
Washington, DC   20375

Chief, Bureau of Medicine & Surgery
Department of the Navy
ATTN: MED 3C33   1
Washington, DC   20372

Commander
Naval Air Systems Command
ATTN: Code AIR-301C (Dr. H. Rosenwasser) 1
ATTN: Code AIR-5363 (D. C. Caldwell)   1
Washington, DC   20361

Commander
Naval Sea Systems Command
ATTN: SEA-62Y13 (LCDR Richard Gilbert)   1
ATTN: SEA-62Y21 (A. Kanterman)   1
ATTN: SEA-62Y21 (LCDR W. Major)   1
Washington, DC   20362

Project Manager
Theatre Nuclear Warfare Project Office
ATTN: PM-23 (Dr. Patton)   1
ATTN: TN-09C   1
Navy Department
Washington, DC   20360

Commander
Naval Surface Weapons Center
Dahlgren Laboratory
ATTN: DX-21   1
ATTN: Mr. R. L. Hudson   1
ATTN: F-56 (Mr. Douglas Marker)   1
Dahlgren, VA   22448

Commander
Naval Intelligence Suport Center
ATTN: Code 434 (H. P. St.Aubin)   1
4301 Suitland Road
Suitland, MD   20390

Commander
Naval Explosive Ordnance Disposal
    Technology Center
ATTN: AC-3   1
Indian Head, MD 20640

Officer-In-Charge
Marine Corps Detachment   1
Naval Explosive Ordnance Disposal
    Technology Center
Indian Head, MD 20640

Commander
Naval Air Development Center
ATTN: Code 2012 (Dr. Robert Helmbold) 1
Warminster, PA 18974

Commander
Naval Weapons Center
ATTN: Code 3893 (L. A. Mathews)   1
ATTN: Code 3882 (Dr. C. E. Dinerman) 1
ATTN: Code 3918 (Dr. Alex Shlanta)   1
China Lake, CA 93555

Commanding Officer
Naval Weapons Support Center
Applied Sciences Department
ATTN: Code 50C, Bldg 190   1
ATTN: Code 502 (Carl Lohkamp)   1
ATTN: Code 5063 (R. Farren)   1
Crane, IN 47522

US MARINE CORPS

Commanding General
Marine Corps Development and
    Education Command
ATTN: Fire Power Division, D091   1
Quantico, VA 22134

DEPARTMENT OF THE AIR FORCE

Department of the Air Force
Headquarters Foreign Technology Division
ATTN: TQTR   1
Wright-Patterson AFB, OH 45433

AFAMRL/TS
ATTN: COL Johnson   1
Wright-Patterson AFB, OH 45433

AFWAL/FIEEC (Wendell Banks)   1
Wright-Patterson AFB, OH 45433

HQ AFSC/SDZ   1
ATTN: CPT D. Riediger
Andrews AFB, MD 20334

USAF TAWC/THL   1
Eglin AFB, FL 32542

USAF SC
ATTN: AD/YQ (Dr. A. Vasiloff)   1
ATTN: AD/YQO (MAJ Owens)   1
Eglin AFB, FL 32542

AD/XRO   1
Eglin AFB, FL 32542

Commander
Hanscom Air Force Base
ATTN: AFGL/LYC (Dr. Barnes)   1
ATTN: AFGL/POA (Dr. Frederick Volz) 1
Bedford, MA 01731

Headquarters
Tactical Air Command
ATTN: DRP   1
Langley AFB, VA 23665

AFOSR/NE
ATTN: MAJ H. Winsor   1
Bolling AFB, DC 20332

OUTSIDE AGENCIES

OSV Field Office   1
P.O. Box 1925
Eglin AFB, FL 32542

Battelle, Columbus Laboratories
ATTN: TACTEC   1
505 King Avenue
Columbus, OH 43201

Toxicology Information Center, JH 652
National Research Council   1
2101 Constitution Ave., NW
Washington, DC 20418

Los Alamos National Laboratory
ATTN: T-DOT, MS B279 (S. Gerstl)   1
Los Alamos, NM 87545

Institute for Defense Analysis   1
1801 N. Beauregard Street
Alexandria, VA 22311

ADDITIONAL ADDRESSEES

Office of Missile Electronic Warfare
ATTN: DELEW-M-T-AC (Ms Arthur)   1
White Sands Missile Range, NM 88002

US Army Mobility Equipment Research and
    Development Center
ATTN: DROME-RT (Mr. O. F. Kezer)   1
Fort Belvoir, VA 22060

Director
US Night Vision and EO Laboratories
ATTN: DRSEL-NV-VI (Dr. R. G. Buser)   1
ATTN: DRSEL-NV-VI (Mr. R. Bergemann)   1
ATTN: DELNV-VI (Luanne Obert)   1
ATTN: DELNV-L (D. N. Spector)   1
Fort Belvoir, VA 23651

Commandant
Academy of Health Sciences, US Army
ATTN: HSHA-CDH   1
ATTN: HSHA-IPM   2
Fort Sam Houston, TX 78234

Science Applications Inc.
ATTN: Dr. Frederick G. Gebhardt   1
3 Preston Court
Bedford, MA 01730

Science Applications Inc.
ATTN: Mr. Robert E. Turner   1
1010 Woodman Drive, Suite 200
Dayton, OH 45432

Creative Optics   1
25 Washington St
Bedford, MA 01730

McDonnell Douglas Astro Co
ATTN: John Adams (A-3-210,11-1)   1
5301 Bolsa Ave
Huntington Beach, CA 92647

BMD Program Office
ATTN: Dick McAtee, Rm. 7S14   1
5001 Eisenhower Ave
Alexandria, VA 22333

Dr. W. Michael Farmer, Assoc Prof, Physics
University of Tennessee Space Institute   1
Tullahoma, TN 37388